

Shock Tube and Theory Investigation of Cyclohexane and 1-Hexene Decomposition

J. H. Kiefer*¹; K. S. Gupte¹, L. B. Harding², S. J. Klippenstein²

¹ University of Illinois at Chicago, Chicago IL 60607

² Argonne National Laboratory, Argonne IL 60439

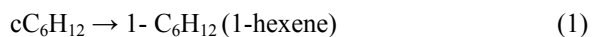
Abstract

The decomposition of cyclohexane (c-C₆H₁₂) was studied in a shock tube using the laser schlieren technique in the temperature range 1400-2000 K and over 25-200 torr in mixtures of 2, 4, 10 and 20% cyclohexane in Kr. The dissociation of 1-hexene, apparently the sole initial product of cyclohexane dissociation, was also studied over 1220-1700 K for 50 and 200 torr using 2 and 3% 1-hexene in Kr. Cyclohexane simply isomerizes to 1-hexene, and this then dissociates almost entirely into allyl radical and n-propyl radical. Rate constants and RRKM parameter fits are provided for the entire range of conditions. Extrapolated high-pressure rates are in good agreement with much of the literature.

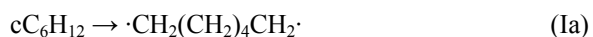
Introduction

Cyclohexane is a common fuel component and a routine surrogate for other naphthenes. As such, its decomposition has been extensively examined, but the actual product channels are still not decided and good rate data are rather limited.

The earliest modern observation of cyclohexane dissociation, at least for the high temperature conditions appropriate to pyrolytic initiation, was made by Tsang¹. His experiments used single pulse shock tube heating together with a GC/FID (flame ionization detector) analysis of stable species and employed the dissociation of a chemical thermometer (cyclohexene) to determine temperature. Tsang determined that the only reaction channel around 1100 K was isomerization to 1-hexene.

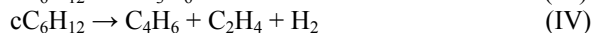


Based on common trends seen in the dissociation of other cycloalkanes, Tsang also proposed a diradical pathway for this as in reactions (Ia) and (Ib)



Tsang also complemented his work on cyclohexane dissociation by a separate study of 1-hexene

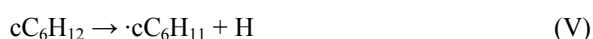
More recently, Aribike, et al.^{2, 3} studied cyclohexane dissociation in an annular flow reactor over 1000-1300 K with 1 atm pressure of N₂ as bath gas. They proposed reactions (II) – (IV).



Tsang's proposed diradical pathway, (Ia) and (Ib), was supported by Brown and coworkers⁴ who studied the dissociation of cyclohexane at temperatures 900-1200 K using the Very Low Pressure Pyrolysis (VLPP) technique. An additional set of experiments were carried out on the dissociation of

vinylcyclohexane. Their estimated k_∞ for 1000 K is a factor of 4 higher than the rate constant reported by Tsang¹

Voisin, et al.,⁵ studied cyclohexane oxidation in a jet stirred reactor for 750-1100 K and 10 atm in cyclohexane/air mixtures at various equivalence ratios. In addition to channel (II) they introduced a C-H fission channel:



El-Bakali, et al.,⁶ also studied cyclohexane oxidation in a jet stirred reactor over 750-1200 K using 1,2 and 10 atm of cyclohexane/air mixtures at different equivalence ratios. A further diradical channel was suggested:



Granata, et al.,⁷ introduced the channel



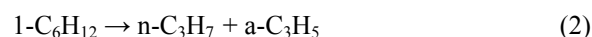
McEnally, et al.⁸ studied cyclohexane pyrolysis in a co-flowing, non-mixed CH₄/air flame doped with 2000 ppm cyclohexane covering 400-2000 K at 1 atm pressure. Based on product analysis, rate expressions were suggested for channels (I), (II) and (V).

Most recently, Braun-Unkoff, et al.,⁹ investigated highly diluted cyclohexane pyrolysis in reflected shock waves using the H-atom ARAS technique to monitor time dependent H-atom concentration for T = 1200-1900 K and P = 1.5-2 bar of argon. Here (II) and (V) were suggested as possible dissociation channels. There are also several other studies of the oxidation that have proposed pyrolytic mechanisms.¹⁰⁻¹⁴

In addition to all the experimental and simulation studies, a theoretical study has been carried out by Sirjean, et al.,¹⁵ using the CBS-QB3 method. They reported that the ring opening in cyclohexane does indeed proceed through formation of a diradical intermediate, as in (Ia). Unimolecular rate constants

were calculated using transition state theory and overall rate constants were then determined by applying a steady-state to the diradical. Recognizing the numerous conformers involved in (Ia) and (Ib), two schemes, labeled 7 and 8, were put forward. In scheme 7, only the lowest energy diradical was considered, neglecting internal rotation barriers, whereas in scheme 8, rotational hindrance in the diradical was explicitly considered. The rates they derived for these are shown below.

Regarding 1-Hexene itself, it mainly dissociates via a rapid C-C fission. As expected, the C3-C4 bond in 1-hexene is weakest, and fission through reaction (2) is supported by Tsang's study of products from 1-hexene dissociation.¹



while the contribution from the retro-ene channel,



to the overall rate is around 10-20%. The latter is discussed again later.

1-Hexene dissociation was also studied by King¹⁶ using the VLPP technique in 915-1153 K, with results in very close agreement with Tsang.

Specific objectives

Our main purpose here is presentation and examination of new experimental results with the intent of establishing the correct reaction paths for the high temperatures involved in pyrolytic ignition. For this 31 laser-schlieren (LS) experiments were carried out on 2% and 3% 1-hexene/Kr mixtures in 1220-1700 K and 50 and 200 Torr, and 131 experiments on 2, 4, 10 and 20% cyclohexane/Kr mixtures in 1400-2000 K and over 25-200 Torr were performed. The LS technique in its present version is fully described in refs. 17 and 18. These experiments used cyclohexane and 1-hexene of high purity from Sigma Aldrich and krypton diluent from Spectra Gases. Calculations assumed ideal-shock, ideal-gas behavior and employed the thermodynamic data of Burcat and Ruscic¹⁹ for all calculations.

Results and Discussion

1-Hexene

The mechanism for 1-hexene decomposition is essentially that of the $\cdot\text{C}_3\text{H}_7$ and $\cdot\text{C}_3\text{H}_5$ dissociations following reaction (2). Where available, rate constants in the mechanism were taken from the literature - especially refs. 20-22. RRKM rate constants for unimolecular reactions were calculated, wherever possible, and if not, the available k_∞ were reduced appropriately for falloff. The procedure for RRKM rate constant calculation is straightforward; TST parameters (vibrational frequencies, rotational constants and reaction barriers) were selected from the literature or calculated using electronic structure

theory (G3B3), with barriers adjusted when necessary so that well established k_∞ were reproduced.

Given the need for concision, the experiments on 1-hexene are not described here in detail. However, the fit to experiment is uniformly excellent and the derived bond-fission rate constants are displayed on the Arrhenius plot of Fig. 1 below. This figure also shows the result of an RRKM fit using a restricted-rotor Gorin model as is appropriate for a bond fission reaction like (2). For this calculation the barrier was 73.74 kcal/mol (G3B3) and $\langle\Delta E\rangle_{\text{down}} = 640 \text{ cm}^{-1}$. It is assumed that appropriate selection of the "restriction parameter" in this calculation will also compensate for any inadequacies in treatment of the internal rotors in the molecule.

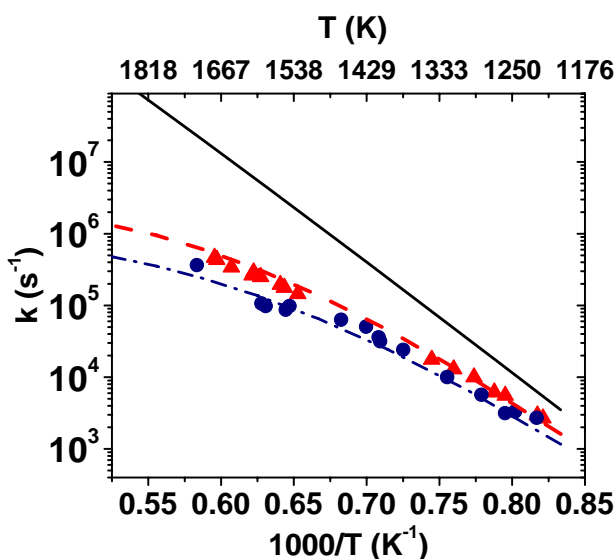


Figure 1: Arrhenius plot of laser schlieren rate constants for 1-hexene dissociation (2). The 50 [●] and 200 [▲] Torr groups contain experiments in the following ranges P=50: (45-67 Torr), P=200: (169-237 Torr). The RRKM fall-off curves for 50 [---], 200 Torr [---] and, the high pressure limit [—] are also shown.

The resulting high pressure limit rate constant for (2) from the RRKM model is

$$k_\infty(2) = 1.46 \times 10^{16} \exp(-69.12 \text{ kcal/mol} / RT) \text{ s}^{-1}$$

($T=1200\text{-}1700 \text{ K}$, $<7\%$ error). This is 3-4 times higher than the k_∞ of Tsang¹. This disagreement is discussed below.

Cyclohexane

An energy diagram for cyclohexane is presented in Fig. 2, constructed using $\Delta H_f^{\circ}{}_{298\text{K}}$ and $H_{298}-H_0$ from Burcat and Ruscic¹⁹ except for energies of the transition states taken from new calculations and the literature¹⁵. Of course if channels (I), (II) and (III) proceed through a diradical, an additional step is involved. Here TS1 is the transition state for reaction (Ia), the energy for which is from CASPT2/cc-pVDZ calculations. The energy of TS4, the transition state for channel (II) is taken from ref. 15. The two transition states, TS1 and TS4, are rate controlling for the reactions (1) (described below) and (II)¹⁵

respectively. $\Delta H_f^{\circ 298K}$ and $H_{298}-H_0$ for the $\cdot C_5H_9$ radical and the energy of TS6 were calculated at the G3B3 level of theory. The TS5 energy shown in Fig. 2 is from a G3B3 calculation.

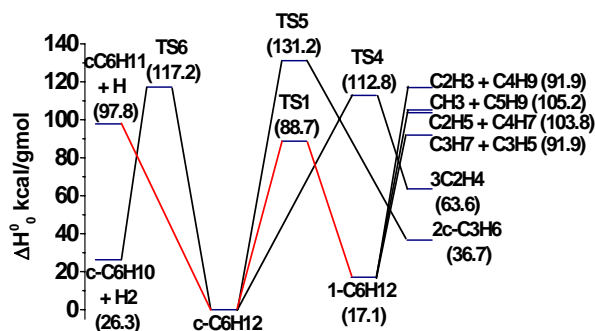


Figure 2: An energy diagram depicting possible cyclohexane dissociation channels with species and TS energies relative to cyclohexane.

We have estimated a k_{∞} for the C-H fission of (V) assuming the rate of the reverse $H + c-C_6H_{11} \rightarrow c-C_6H_{12}$ is the same as that of the reaction $H + iso-C_3H_7 \rightarrow C_3H_8$ taken from ref. 23, with the result $k_{\infty}(V) = 6.8 \times 10^{15} \exp(-97.0/RT)$. This is not competitive, and has thus been ignored.

Example LS experiments on cyclohexane are shown in the semilog gradient plots of Figs. 3-6. As illustrated in the example attempt to model the experiments of Fig. 3 with reaction (II), the gradient observed in the LS experiments cannot in fact be modeled with a major contribution from any of the molecular channels (II), (III), (IV) or (VI). This is simply because the endothermicity resulting from these is small and adequate at any time as the products are also quite stable and do not dissociate. We conclude that none of the proposed molecular channels make a significant contribution to the overall dissociation rate, even for the highest temperatures used herein.

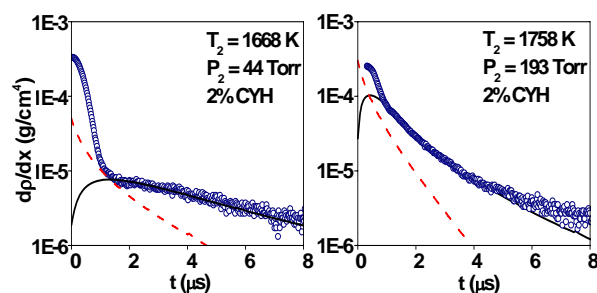


Figure 3: Comparison between density gradients generated by the two possible channels (1) and (II). The solid line is generated using only (1) as the cyclohexane dissociation channel, including the mechanism for the dissociation of the 1-hexene product, whereas the dotted line is generated using (II) as the sole cyclohexane dissociation channel.

Having all the decomposition through (1) alone is also supported by the previous experimental work of Tsang¹ and Brown, et al.⁴. Moreover, the ‘two-step’ process of (1) followed by (2) and further reactions of the 1-hexene decomposition produce the upward curvature fully resolved in Fig. 4, and this is a defining characteristic of the ‘two-step’ process. The initial step of cyclohexane dissociation (1) is 19 kcal/mol endothermic, whereas the dissociation of the product 1-hexene through reaction (2) is not only faster but 75 kcal/mol endothermic. The decomposition of its allyl and n-propyl products now increases this even further. Of course at $t=0$, only the cyclohexane isomerization contributes to the density gradient. The small gradient generated by this then rises strongly as 1-hexene is formed and rapidly dissociates. After a short time, the density gradient profile reaches a maximum which roughly corresponds to a steady state in the 1-hexene. At later times, the gradient drops again from temperature drop and depletion.

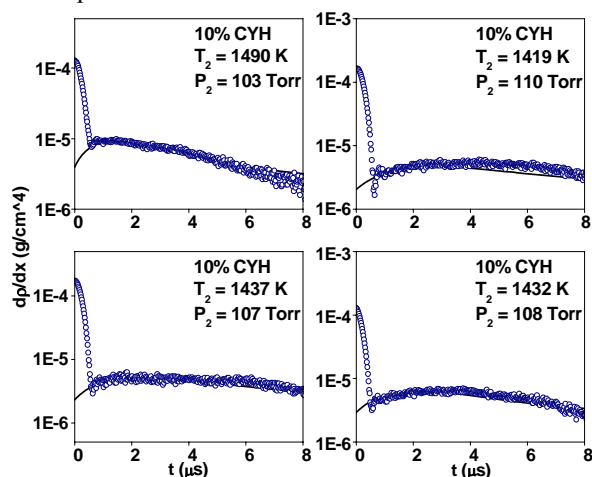


Figure 4: Semilog plots of curved density gradient profiles produced by pyrolysis of cyclohexane/Kr mixtures at the indicated temperatures and pressures. The open circles [○] are the measurements and the solid lines in these figures are simulations generated by the ‘two-step’ process of (1) and (2).

We conclude, on the basis of Figs. 3 and 4, that 1-hexene is the only significant product of the initial reaction. Here the modeling used the RRKM derived rate constants for (2) at different pressures and the combination of (1) and (2) produced an excellent fit to the experiments. However, in addition to all the 1-hexene reactions, it is now also necessary to include various abstraction reactions involving cyclohexane and the 1-hexene chain radicals, especially H and CH_3 .

Rate constants for H-atom abstraction from cyclohexane were determined theoretically, and those for abstraction by CH_3 and the other rates were estimated using six times the known rate constant for abstraction from the $-CH_2-$ group of propane. Subsequent cyclohexyl decomposition was treated using rates from ref. 24.

In all modeling of the cyclohexane dissociation experiments exhibited here, only the rate of reaction (1) (or (1a) for the 25 Torr experiments; see below) was adjusted. To deal with falloff, different mechanisms were used for modeling the 25, 50, 100, 150 and 200 Torr experiments. The “two-step” model whose results are shown as the solid lines in Figs 3-6., has (1) followed by (2), in contrast to the “one-step” model shown by the dashed lines in Fig. 6, where reactions (1) and (2) are combined into a single reaction (1a). These two models are described in detail just below.

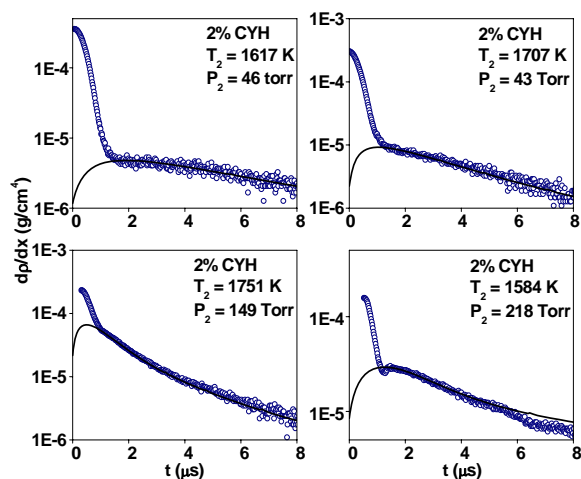


Figure 5: Semilog density gradient profiles showing cyclohexane dissociation in cyclohexane/Kr mixtures for the indicated temperature, pressure and composition having unresolved maxima. The solid lines in these figures are simulations generated with the ‘two-step’ process.

The cyclohexane energy diagram in Fig. 1 suggests that the energies of TS1 and the $C_3H_7 + C_3H_5$ fission channel are very close. It is then entirely possible that at low pressures (lower rate of collisional deactivation) and/or at high temperatures (higher excitation energies), cyclohexane will dissociate via the ‘one-step’ reaction (1a) through chemically activated 1-hexene directly producing C_3H_7 and C_3H_5 radicals. That is, the intermediate 1-hexene is not stabilized, and the previous maxima in gradient of Fig. 4 will no longer appear.



A few extremely low pressure (~25 Torr), high temperature experiments do somewhat indicate a dominance of this process as seen in Fig. 6.

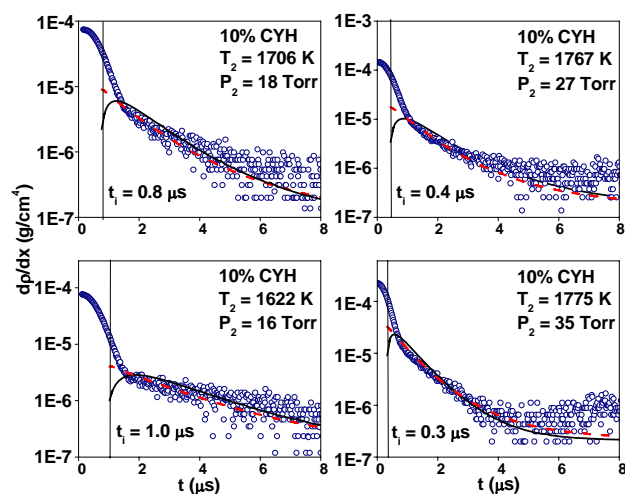


Figure 6: Semilog plots of density gradient profiles produced by pyrolysis of cyclohexane/Kr mixtures at the indicated high temperatures and very low pressures. The solid and dotted lines in these figures are simulations generated with ‘one-step’ and ‘two-step’ processes respectively.

Because of their extremely low pressures, the Fig. 6 experiments present unique problems. Inasmuch as relaxation in cyclohexane can hardly be instantaneous, it was necessary to recognize the possibility of incubation delays in the modeling for such low pressures. To deal with this we have measured relaxation times in cyclohexane in some very low P and T experiments (<20 Torr, 1100-1500 K). The resulting times are very short and nearly constant at $P\tau = 62$ nsec-atm. Incubation times (t_i) could not be determined, and were then estimated using the t_i/τ ratios seen in neopentane. As seen in Fig. 6 the flat gradients generated by the ‘one-step’ model (1a) now provide a slightly superior fit as compared to the ‘two-step’ model, and thus all the 25 Torr experiments were modeled using reaction (1a) instead of (1). However, this is actually of little practical consequence; the rate constants required for reaction (1) and (1a) differ only by 20%, less than the experimental uncertainty.

Again, in all modeling of the cyclohexane dissociation experiments exhibited here, only the rate of reaction (1) (or (1a)) was adjusted. To deal with falloff, different mechanisms were used for modeling the 25, 50, 100, 150 and 200 Torr experiments.

The derived rate constants for cyclohexane dissociation from all the fitted experiments are displayed on the Arrhenius plot of Fig. 5. The lines shown on the plot are from a RRKM treatment of cyclohexane dissociation described below.

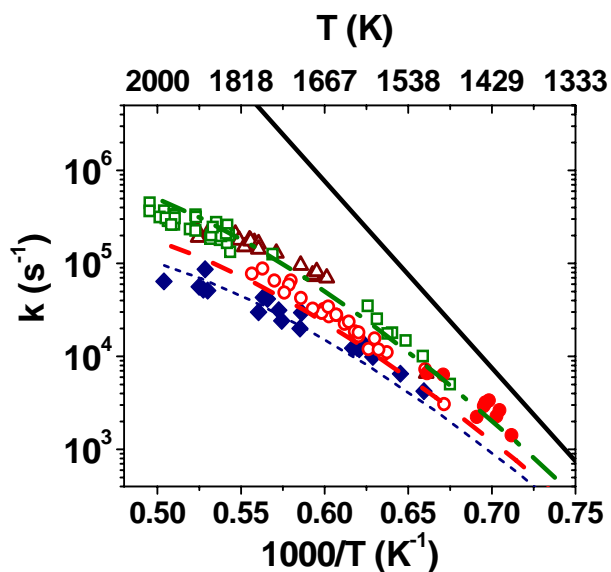


Figure 7: Arrhenius plot of rate constants for cyclohexane dissociation (1). The 25 [◆], 50 [○], 100 [■], 150 [△] and 200 [□] Torr groups contain experiments in the following ranges P=25: (16-35 Torr), P=50: (38-67 Torr), P=100: (97-123 Torr), P=150: (144-162 Torr), P=200: (185-233 Torr). The RRKM fall-off curves for 25 [---], 50 [---], 200 Torr [- · - · -] and, the high pressure limit [—] are also shown.

Theory

Here theory consists in some electronic structure calculations and applications of RRKM theory. Energetics for channels (1), (Ia) and (Ib), calculated at the CASPT2/cc-pVDZ level are shown in Fig. 2. An interesting added feature discovered in these calculations is a transition state which takes isomerization of cyclohexane to 1-hexene directly without formation of a diradical intermediate. Although the barrier to this is lower than the ring opening barrier TS1, this direct step is not favored because of its lower entropy of activation.

An accurate RRKM treatment for predicting falloff in the cyclohexane dissociation is complicated by various factors. For one thing, the diradical of (Ia) has several conformational forms which need to be considered. An approximate theoretical treatment was used to deal with this problem. The ring opening of cyclohexane was taken to be the sole rate controlling step and the direct isomerization above, was considered minor. Hence a vibration model RRKM theory, using a transition state for (Ia), was used for falloff calculations



The harmonic frequencies of the cyclohexane chair structure (#1 in Sirjean, et al.,¹⁵) and of the transition state for (Ia) were scaled by 0.99 as per the recommendation also given in ref. 15. Moments of

inertia of cyclohexane and the TS were also obtained from ref. 15 with their lowest moments considered active and the remainder adiabatic²⁵. The barriers for the ring opening process from ref. 15 and at the CASPT2/cc-pVDZ level of theory were 88.8 kcal/gmol and 88.7 kcal/gmol respectively. These calculated barriers failed to fit the rates at high temperatures so the barrier was reduced to 86.0 kcal/mol. Also part of this fit was a $\langle \Delta E \rangle_{\text{down}}$ of 600 cm^{-1} . The resulting high-pressure rate constant is $k_{\infty}(1) = 8.76 \times 10^{17} \exp(-91.94 \text{ kcal/gmol} / RT) \text{ s}^{-1}$ (T-1300-2000 K, <1% error).

A comparison of k_{∞} values for cyclohexane dissociation (1) is given in Fig. 8. The present RRKM k_{∞} is in very close agreement with the preferred k_{∞} of scheme 8 reported by Sirjean, et al.¹⁵ and also with the rate of King, et al.,⁴ but is again, as in 1-hexene, almost 3-4 times higher than that of Tsang¹. We believe this disagreement results from some remaining falloff in Tsang's experiments and likely problems with his temperature determination²⁶.

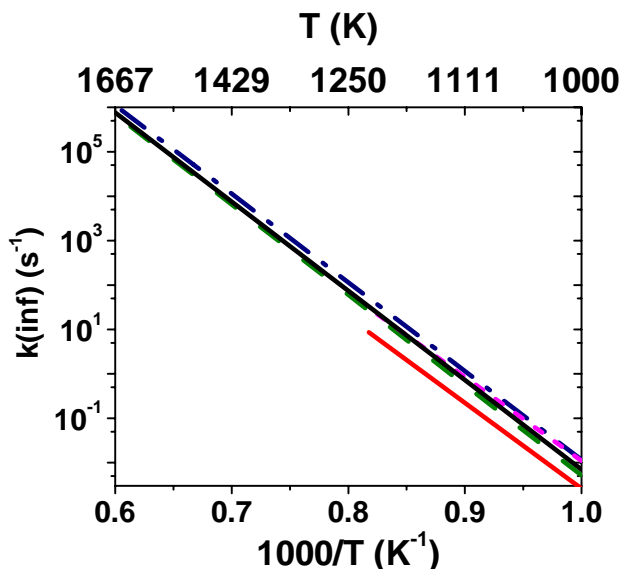


Figure 8: Comparison with the literature high pressure limit rate constants for cyclohexane dissociation. [—]: Present work (RRKM); [—]: Tsang¹; [---]: Brown, et al.⁴; [- · - · -]: Sirjean, et al. Scheme 7 in ref. 15; [---]: Sirjean, et al. Scheme 8 in ref. 15

Conclusions

This study has measured accurate ($\pm 30\%$) rate constants of 1-hexene and cyclohexane dissociation at high temperatures and low pressures. The sole significant initial channel for cyclohexane decomposition is isomerization to 1-hexene which then dissociates rapidly into allyl and n-propyl radicals. Any contributions from other possible molecular channels are certainly very minor in cyclohexane.

The rate constants for both decomposition reactions are deep into falloff at the present high temperatures and k_{∞} were estimated by RRKM extrapolation. The resulting k_{∞} are in close agreement

with one experimental datum⁴ and the theoretical k_{∞} by Sirjean, et al¹⁵. Disagreements with the k_{∞} of Tsang¹ are probably a consequence of residual falloff and perhaps some error in his comparison rates.

Acknowledgements

This work was supported by the U.S. Department of Energy, Office of Basic Energy Sciences, Division of Chemical Sciences, Geosciences and Biosciences under grant no. DE-FE-85ER13384 (J. K and K. G.), and under contract number DE-AC02-06CH11357 (S. J. K and L. B. H.).

References

1. W. Tsang, Int. J.Chem.Kinet. **1978**, 10, (11), 1119-1138.
2. D. S. Aribike; A. A. Susu; A. F. Ogunye, Thermochimica Acta **1981**, 51, (2-3), 113-127.
3. D. S. Aribike; A. A. Susu; A. F. Ogunye, Thermochimica Acta **1981**, 47, (1), 1-14.
4. T. C. Brown; K. D. King; T. T. Nguyen, J. Phys. Chem. **1986**, 90, (3), 419-24.
5. D. Voisin; A. Marchal; M. Reuillon; J. C. Boettner; M. Cathonnet, Comb. Sci. and Tech. **1998**, 138, (1-6), 137-158.
6. A. El-Bakali; M. Braun-Unkhoff; P. Dagaut; P. Frank; M. Cathonnet, Proc. Comb. Inst. **2000**, 28, 1631-1638.
7. S. Granata; T. Faravelli; E. Ranzi, Comb. Flame **2003**, 132, (3), 533-544.
8. C. S. McEnally; L. D. Pfefferle, Comb. Flame **2004**, 136, (1-2), 155-167.
9. M. Braun-Unkhoff; C. Naumann; P. Frank, Abs. Paps. Amer. Chem. Soc. **2004**, 227, U1096-U1096.
10. M. E. Law; P. R. Westmoreland; T. A. Cool; J. Wang; N. Hansen; C. A. Taatjes; T. Kasper, Proc. Comb. Inst. **2007**, 31, 565-573.
11. H. Z. R. Zhang; L. K. Huynh; N. Kungwan; Z. W. Yang; S. W. Zhang, J. Phys. Chem. A **2007**, 111, (19), 4102-4115.
12. B. Sirjean; F. Buda; H. Hakka; P. A. Glaude; R. Fournet; V. Warth; F. Battin-Leclerc; M. Ruiz-Lopez, Proc. Comb. Inst. **2007**, 31, 277-284.
13. E. J. Silke; W. J. Pitz; C. K. Westbrook; M. Ribaucour, Comb. Flame mistry A **2007**, 111, (19), 3761-3775.
14. O. Lemaire; M. Ribaucour; M. Carlier; R. Minetti, Comb. Flame **2001**, 127, (1-2), 1971-1980.
15. B. Sirjean; P. A. Glaude; M. F. Ruiz-Lopez; R. Fournet, J. Phys. Chem. A **2006**, 110, (46), 12693-12704.
16. K. D. King, Int. J. Chem. Kinet. **1979**, 11, (10), 1071-1080.
17. J. H. Kiefer; A. C. Manson, Rev. Sci. Inst. **1981**, 52, (9), 1392-1396.
18. J. H. Kiefer, in: *Shock Waves in Chemistry*, A. Lifshitz, (Ed.) Marcel Dekker: New York, 1981; pp 219-277.
19. A. Burcat; B. Ruscic, in: Ideal Gas Thermochemical Database with updates from Active Thermochemical Tables 2008. <ftp://ftp.technion.ac.il/pub/supported/aetdd/thermodynamics>.
20. W. Tsang, Ind. Eng. Chem. Res. **1992**, 31, (1), 3-8.
21. W. Tsang; R. F. Hampson, J.Phys. Chem. Ref. Data **1986**, 15, (3), 1087-1279.
22. D. L. Baulch; C. J. Cobos; R. A. Cox; C. Esser; P. Frank; T. Just; J. A. Kerr; M. J. Pilling; J. Troe; R. W. Walker; J. Warnatz, J.Phys. Chem. Ref. Data **1992**, 21, (3), 411-734.
23. L. B. Harding; Y. Georgievskii; S. J. Klippenstein, J. Phys. Chem. A **2005**, 109, (21), 4646-4656.
24. I. Iwan; W. S. McGivern; J. A. Manion; W. Tsang, Proc. 5th US Comb. Meet., San Diego, CA **2007**, CO2.
25. W. Forst, "Unimolecular reactions: a concise introduction". Cambridge University Press: Cambridge, U.K. ; New York, 2003.
26. Kalra, B. L.; Feinstein, S. A.; Lewis, D. K., Can. J. Chem. 1979, 57, (11), 1324-1328.